Ultra-low molecular weight photoswitchable hydrogelators

Fayaz Ali Larik,[a,b] Lucy L. Fillbrook,[a] Sandra S. Nurttila,[a,b] Adam D. Martin,[c] Rhiannon P. Kuchel,[d] Karrar Al Taief,[a,b] Mohan Bhadbhade,[e] Jonathon E. Beves*[a] and Pall Thordarson*[a,b]

[a]   F. A. Larik, L. L. Fillbrook, Dr. S. S. Nurttila, K. Al Taief, Dr. J. E. Beves, Prof. Pall Thordarson
       School of Chemistry
       The University of New South Wales
       Sydney, NSW 2052, Australia
       E-mail: j.beves@unsw.edu.au and p.thordarson@unsw.edu.au
[b]   F. A. Larik, Dr. S. S. Nurttila, K. Al Taief, Prof. Pall Thordarson
       The Australian Centre for Nanomedicine and the ARC Centre of Excellence in Convergent Bio-Nano Science and Technology
       The University of New South Wales
       Sydney, NSW 2052, Australia
[c]   Dr A. D. Martin
       Dementia Research Centre, Department of Biomedical Science, Faculty of Medicine and Health Sciences
       Macquarie University
       Sydney, NSW 2109, Australia
[d]   Dr. R. P. Kuchel
       Electron Microscopy Unit, Mark Wainwright Analytical Centre
       The University of New South Wales
       Sydney, NSW 2052, Australia
[e]   Dr. M. Bhadbhade
       Solid State & Elemental Analysis Unit, Mark Wainwright Analytical Centre
       The University of New South Wales
       Sydney, NSW 2052, Australia

       Supporting information for this article is given via a link at the end of the document

Abstract: Two photoswitchable arylazopyrozoles form hydrogels at a concentration of 1.2% (w/v). With a molecular weight of 258.28 g/mol, these are the lowest known molecular weight hydrogelators that respond reversibly to light. Photoswitching of the *E*- to the *Z*-form by 365 nm light results in a macroscopic gel→sol transition; nearly an order of magnitude reduction in the measured elastic and loss moduli. In the case of the *meta*-arylazopyrozole, cryogenic transmission electron microscopy suggests that the 29±7 nm wide sheets in the *E*-gel state narrow to 13±2 nm upon photoswitching to the predominantly *Z*-solution state. Photoswitching for *meta*-arylazopyrozole is reversible through cycles of 365 nm and 520 nm excitation with little fatigue. The release of a Rhodamine B dye encapsulated in gels formed by the arylazopyrozoles is accelerated more than 20-fold upon photoswitching with 365 nm light, demonstrating these materials are suitable for light-controlled cargo release.

Introduction

The formation of cytoskeletal filaments[1] and flagellar filaments of bacteria[2] rely on the self-assembly of smaller components. Synthetic small molecules have also been shown to self-assemble in water to form structures ranging from the nanometer scale to micrometer scale,[3] with hydrogelators[4] being one example. Controlling the self-assembly of hydrogels using external stimuli has been challenging[5] but can be achieved by introducing the appropriate responsive units within the molecular components of these systems.

Hydrogel research[4] has evolved from static materials to dynamic smart materials. Controlling the mechanical, physical and chemical properties of hydrogels with external stimuli is important for both medical and industrial uses such as controlled drug delivery,[6] sensing,[7] robotics[8] and 3D cell cultures.[9] Light

has a clear advantage due to its ability to operate in a highly precise manner without contaminating samples.[10] Hydrogels have been made light responsive by the inclusion of a light responsive photoswitchable unit in the gelator molecule.[10c,10d] All previous examples have relied on the inclusion of peptides or other additional groups to enable hydrogel formation (Figure 1a,b). Peptide-[11,10c,10d] or polymer-based[12] hydrogels have been rendered photoresponsive by introducing molecular photoswitches such as diarylethene,[13] spiropyran,[11,14a,10d,14b] azobenzene,[15a-l,10e,15m,15n] stilbene,[16] *ortho*-fluoroazobenzenes,[17] and arylazopyrazoles.[18,12c]

Arylazopyrazoles (AAP) are a recently introduced class of azohetereoarene photoswitches.[19] Azoheteroarenes[19c] are related to azobenzenes but differ as one of the phenyl rings of conventional azobenzene is replaced with heteroarene ring. The Fuchter group has extensively studied these compounds showing almost complete photoisomerization in both directions with the thermal half-life of the metastable *Z*-isomer being tunable from hours to 10 days.[19] Ravoo and co-workers[20] have used arylazopyrazoles to form light responsive gels where a central linker is connected to three photoswitching groups (Figure 1b, MW=1195.27 g/mol). Tetrapeptides gelators (Fmoc-RGDS) were combined with an arylazopyrazole photoswitching unit attached *via* a linker chain (Fmoc-RGDS-AAP).[20]

Most gelators reported in literature, including all photoswitchable gelators, have a MW > 300 g/mol. The bulk of light-responsive gelators contain long alkyl chains, peptides, or polymers and hence the photoswitchable unit plays a secondary role in the self-assembly of these systems. Herein we introduce the first gelators with a molecular weight below 300 (MW= 258.28 g/mol – making it one of smallest hydrogelator reported[21]) that form stable hydrogels at physiological pH and respond to light in a bidirectional way (Figure 1c,d).
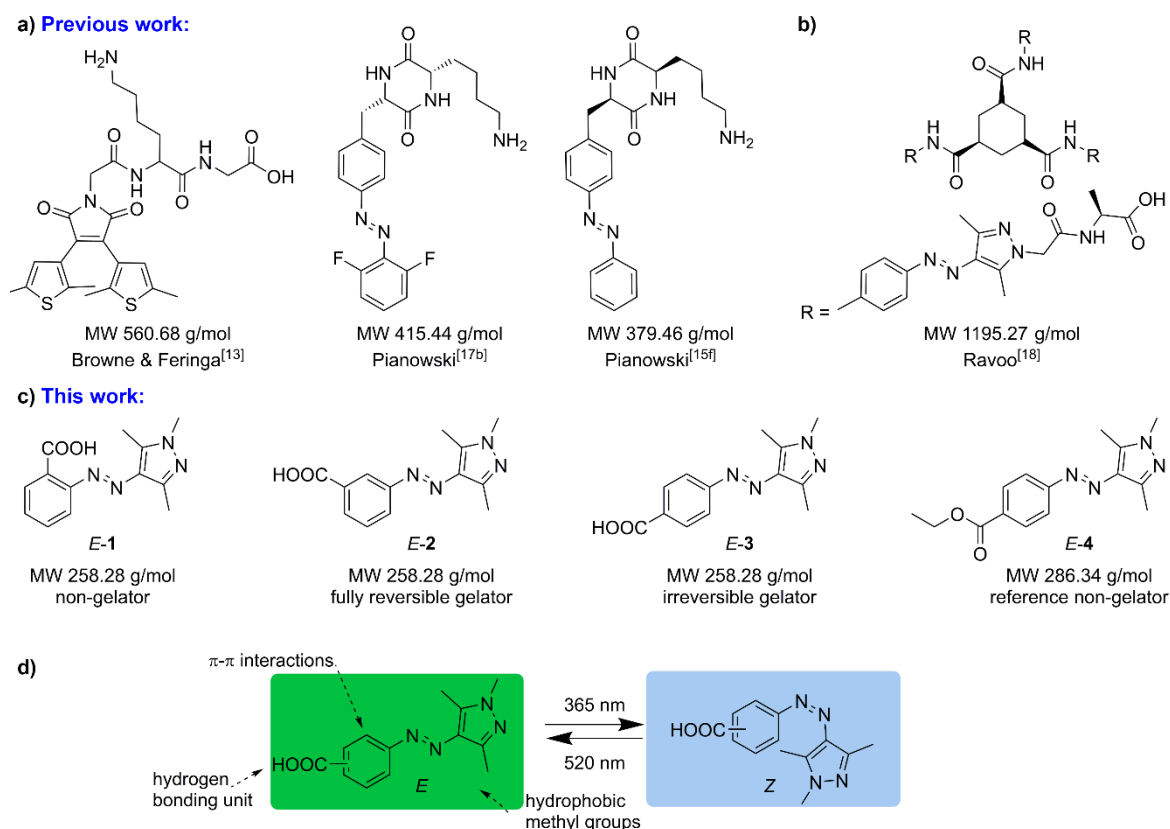
Figure 1. a) The three smallest photoswitchable single-component hydrogelators reported to date. b) The smallest single-component arylazopyrazole photoswitchable gelator previously reported. c) The low molecular weight photoswitching arylazopyrazole compounds **1–4** (in their *E*-form) reported in this work. Compounds **2–3** (MW 258.28 g/mol) form gel in water at 1.0% (w/v), while **1** and control compound **4** do not form gels reported here. d) The design and switching mechanism of low molecular weight photoswitchable gelators **1–3**.

Arylazopyrazole photoswitches **1–3** (Figure 1c) are isomers that differ only in the substitution of the carboxylic acid group on the aromatic ring. The carboxylic acid group can act as a hydrogen bond donor and acceptor, and the pyrazole ring and the diazo nitrogens can act as hydrogen bond acceptors to aid the gelation process. The photoswitches **2** and **3** form hydrogels as a result of intermolecular hydrogen bonding and hydrophobic effects, and represent the minimal non-covalent interactions usually required to trigger gelation. The arylazopyrazole photoswitch **4** bears an ester group at the para position and is used as a control compound not capable of intermolecular hydrogen bonding and hence does not form a gel.

Results and Discussion

Synthesis of photoswitches 1–4

Compounds **1–4** were synthesized using modified literature procedures of related compounds.[19b] The *ortho*-, *meta*- or *para*-aminobenzoic acid and ethylaminobenzoate were reacted with hydrochloric acid and sodium nitrite to form the diazonium salt, which was reacted with acetylacetone to obtain pentane-2,4-diones (**S1–S4**) intermediates (see full characterization in SI-2, SI-12, SI-13, analytical methods described in SI-3). The intermediates (**S1–S4**) were refluxed for 3 h with *N*-methylamine

and then concentrated under reduced pressure to obtain **1–4** as yellow solids in quantitative yields.

The photoswitching behavior of **1–4** was evaluated by UV-vis absorption (SI-4) and NMR spectroscopy (SI-12). Photoswitching using UV-vis absorption was recorded in a range of solvents (DMSO, CH_2Cl_2, methanol, THF, ethyl acetate, chloroform, toluene and acetonitrile) and the spectra in water are shown in Figure 2a. No significant solvatochromism was observed between the eight solvents that were studied (Table S2-S5). The samples were irradiated with 365 nm and 520 nm LED light sources for ~2 min to generate photostationary states (PSS) enriched in the *Z*- or *E*-isomer, labelled PSS_Z and PSS_E respectively. The data is in agreement with that observed for related arylazopyrazole compounds.[19b]

The PSS compositions were quantified by ^1H NMR spectroscopy. The ^1H NMR spectra in DMSO-d_6 of samples equilibrated in the dark showed a single isomer in each case, the expected thermodynamically stable *E*-isomer (see SI-12.9, SI-12.16, SI-12.23 and SI-12.27). The samples were irradiated with 365 nm light for 60 min and ^1H NMR spectra were recorded to obtain the PSS distribution (PSS_Z ≈ 90% Z for each of **1–4**, see SI-12.11, SI-12.18, SI-12.25, SI-12.29). Each sample was then irradiated with 520 nm light to produce a new photostationary state (PSS_E ≈ 92% Figure 2c). The PSS_Z is thermally stable at 25 °C in water over the time scale relevant to all the studies in this work with an

2

apparent half-life measured by UV-vis absorption of 29–34 h for compounds **1**–**4** (Figures S7, S12, S17, S22) All the compounds showed excellent photoswitching behavior in water and DMSO-d_6.
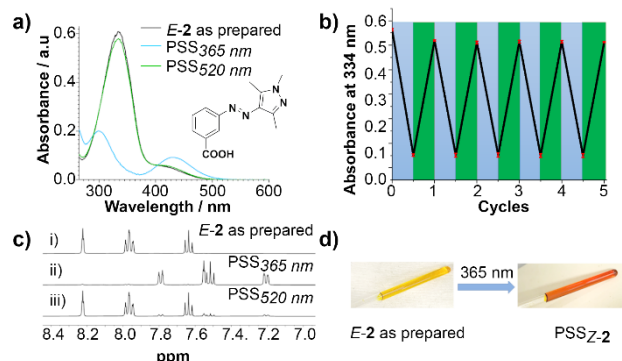

Figure 2. Photoswitching of **2** monitored by a) UV-vis absorption spectra in water of *E*-**2** as prepared (black line) and at photostationary states upon irradiation with 365 nm (blue line) and 520 nm (green line) light. b) Reversible switching of absorption in water monitored at 334 nm upon alternating irradiation with UV (365 nm, indicated with blue) and green (520 nm) light (red error bars = ±1 std from *n* = 3 measurements). c) ¹H NMR (400 MHz, DMSO-d_6) of i) as prepared *E*-**2**, ii) after irradiation with UV (365 nm) or iii) green (520 nm) light. d) NMR tube of *E*-**2** in DMSO-d_6 as prepared and PSS$_Z$ obtained after irradiation with 365 nm light. See Figure SI-4, SI-12 for similar data on **1**, **3** and **4**.

Solid state interactions

Crystals suitable for single crystal X-ray diffraction were grown of **1**–**4** from saturated solutions in DMF/diethyl ether, DMSO and ethanol (SI-6 for details). The structure of **1** showed an intramolecular hydrogen bond between the carboxylic acid group and the adjacent diazo nitrogen (O···N = 2.595(7) Å). Compound **2** is slightly twisted, with an angle of 20.1° between the least-squares planes of the phenyl- and the pyrazole rings. By comparison compound **3** is almost completely flat, with the same angle between the two rings being just 5.39°. The structures of both **2** and **3** show inter-molecular hydrogen bonds between the carboxylic acid group and the free pyrazole nitrogen of an adjacent molecule, with short and similar N···O distances (2.712(4) and 2.689(2) Å, respectively. In each case the hydrogen bonds result in 1D chains that are self-assembled by π-π interactions (centroid-to-plane distances of 3.34 Å and 3.30 Å for **2** and **3** respectively, see Figure 3b, d and Table 1). Details for the structures of **1** and **4** are given in SI-6.

Hirshfeld surface analysis[22] is a powerful tool for visualizing short and long contacts within crystal structures. The so-called "fingerprint" plots of **2**–**3** (SI-7) are superficially very similar, highlighting the importance of the two intermolecular shorts contacts show in Figures 3a and 3c. However, the Hirshfeld fingerprint of **3** highlights a significant pairwise intermolecular H···O interaction between the carbonyl oxygen and an aromatic *meta*-hydrogen on a neighboring molecule. This suggests why gelator **3** packs in an antiparallel fashion in the single crystal structure, in contrast to gelator **2**. Previous studies have shown similar pair-wise interaction drive the formation of antiparallel stacked aromatic molecules.[23] No significant intermolecular short contacts were observed in the Hirshfeld fingerprint plot of **1**
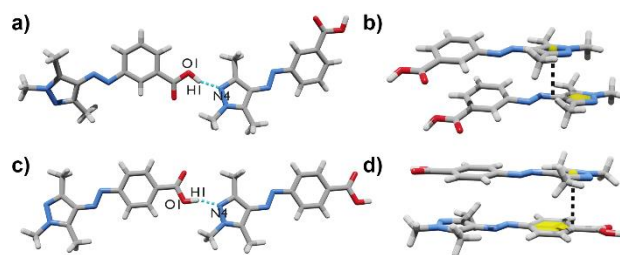

Figure 3. Single crystal X-ray structures of a-b) **2** and c-d) **3**. The *ortho* derivative 1 has an intramolecular hydrogen bond and does not form extended chains (SI-6.5). Both the *meta*-**2** and *para*-derivatives **3** form 1D hydrogen bonded chains as shown. Centroid-to-plane distances are shown with black dotted lines.

Table 1. Comparison of the key parameters of hydrogen bonding of isomers **1**–**3**, obtained from the single crystal X-ray diffraction data.

Inter/Intra	**1** Intra-	**2** Inter-	**3** Inter-
O-H / Å	0.840	0.98(4)	0.94(2)
H···N / Å	1.822	1.774	1.793
O···N / Å	2.595(7)	2.712(4)	2.689(2)
O-H···N / o	152.3	160(4)	160(2)

(Figure S70) due to the intramolecular hydrogen bond between the carboxylic acid and the diazo nitrogen.

Hydrogel formation

Gelation was investigated using the pH switch method with glucono-δ-lactone (gδL).[24] All the starting materials were in the pure *E*-form and these experiments were carried out in the absence of light. Compounds **2** and **3** were dissolved at pH 11, followed by the addition of gδL. After standing at room temperature overnight, hydrogels were formed as determined by the inverted vial test (see SI-9). The minimum gelation concentration for both gelators was determined to be 1.0% (w/v), however, to ensure better consistency in gel properties, all subsequent studies were carried out at 1.2% (w/v) concentration of **2** and **3**. The kinetics of gelation of compounds **2** and **3** was monitored by ¹H NMR spectroscopy (see SI-11). The disappearance of the ¹H NMR signals of the monomeric gelator over ~80 min for **2** or **3** was consistent with aggregation. Compound **1**, which does not form any intermolecular hydrogen bonds in the solid state, does not form a gel in water (SI-8.1). Compound **4**, which also does not display any solid-state intermolecular hydrogen bonding interactions (SI-6.8), does not form a gel. The pK_a values of compound **1**–**3** are practically indistinguishable (determined by pH titrations, see SI-10) with pKa values of 6.4, 6.4 and 6.7 for **1**, **2** and **3**, respectively.

The viscoelastic properties of gels formed by **2** and **3** were studied using a rheometer (Table 2, SI-3). In the dark, the gel formed by **2** was stiffer (elastic modulus G' ~10 kPa) than that of **3** (G' ~1.2 kPa); both were prepared by the pH switch method using gδL (1.2% (w/v); dissolved in 0.1 M sodium hydroxide, followed by the addition of gδL, see SI-3). The frequency sweeps (SI-8.4-8.5) showed that the storage modulus is

independent of the applied frequencies up to ≈10 Hz with some frequency hardening observed at higher frequencies. The strain sweep (SI-8.2) for both **2** and **3** showed that both hydrogels possess malleable-like characteristics, with the linear viscoelastic region lasting until about 10% strain for both gelators. Further increases in strain result in gel collapse at about 60% and 80% strain for **2** and **3**, respectively.

Table 2. Key physical properties of gels formed by **2** and **3** in the dark.

Gelator	mgc[a]	G' [b]	LVR [c]	Fiber diameter[d]
2	1% (w/v)	10 kPa	10%	12.2±0.5 nm
3	1% (w/v)	1.2 kPa	9.5%	13.4 ±0.6 nm

[a] Minimum gelation concentration (mgc). [b] Elastic modulus (G') at strain = 1%, frequency = 1 Hz and 1.2% (w/v) concentration. [c] Elasticity (strain) or linear viscoelastic region (LVR) at frequency = 1 Hz. [d] Histograms of the fiber heights obtained from AFM microscopy and measured for **2** and **3** before irradiation with light. The histograms represent 25 measurements in four different areas for each sample (bin size = 100).

We postulate here that the approximately one order of magnitude difference in the elastic modulus of gels formed by **2** and **3** in the dark can be explained with reference to the observed parallel versus anti-parallel packing in the single crystal structures of **2** and **3**, respectively. Powder X-ray diffraction of xerogels formed from **2** and **3** yielded patterns similar to those predicted from the single crystal X-ray structures (SI-6.11, SI-6.12). The single crystal X-ray structure data and Hirshfeld surface analysis in turn indicate that pairwise intermolecular H⋯O interactions drive the slightly less compact packing of **3** in an antiparallel orientation.

Gel→Sol Photoswitching

Immediately after the addition of gδL, 1.2% (w/v) solutions of **2** and **3** were cast onto a rheometer fitted with a glass plate and allowed to form hydrogel in dark over ~85 min. Dynamic *in situ* time sweep rheological measurements were conducted on **2** and **3** upon exposure to alternating 365 nm and 520 nm light. As the illuminated area is significantly smaller than the diameter (25 mm) of the rheometer measurement plate, the ≈ 500 μL gap was only filled with ca 20% (110 μL) of the gel solution. The absolute elastic (G') and loss (G'') module obtained are therefore not directly comparable to the rheological data obtained under standard conditions in the dark discussed above (see SI-3.8 for further information).

Upon the first irradiation with 365 nm UV light, G' for **2** decreased from about 200 Pa to about 50 Pa over a period of 1 h (Figure 4). Subsequent irradiation of **2** with 520 nm green light restored the initial elasticity of **2** (see Figure 4a). Both green and UV light-irradiated states retained stable G' values for at least 15 min after the light was switched off. Multiple photoswitching cycles were performed on **2** by alternating between UV and green light irradiation and minimal fatigue was observed.

While a gel→sol transition appears to have occurred using a conventional inversion test on **2** (Figure 4) and **3** (Figure S76), the tan δ (the G''/G' ratio) remains well below 1—the conventional rheological definition of a gel[4b]—during the entire course of the light-switching experiments (Figure S75). Strong arguments have been made in the literature that a tan δ < 1 is a more reliable indicator of gelation than the inversion test, albeit

that argument is usually in the situation whereby the materials appears to pass the inversion test while tan δ > 1.[4b, 25] Here, the opposite situation was observed, which is in line with recent observation by Adams and co-workers who attribute this phenomena to the formation of a structured liquid[26] (a liquid with some remaining solid-like rheological properties), but further work is required to explain why irradiation of **2** and **3** leads to an apparent gel transition despite the fact that tan δ < 1.
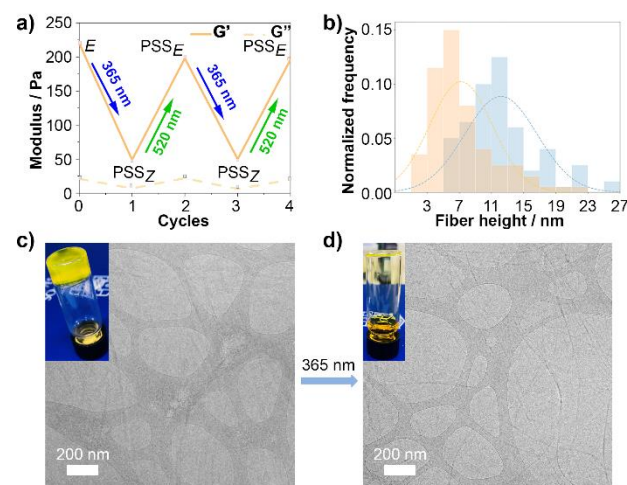

Figure 4. Photoswitching of **2** by alternating irradiation with 365 nm and 520 nm light. Changes in a) rheology with in situ irradiation and b) Size of fibers obtained from AFM microscopy before (blue) and after irradiation (orange) after drop casting dilute (0.0006%, w/v) solution of **2** on to a mica surface. Morphology of fibers obtained from cryo-TEM microscopy of gels formed from **2** in water (1.2% (w/v)) c) before light and d) after irradiation with 365 nm light, scale bar is 200 nm. For the analogous data for compound **3**, see SI-5.3.6 and SI-8.4.

Microscopy studies of gel morphology

Atomic force microscopy (AFM) measurements were conducted starting with 1.2% (w/v) solutions of **1**–**4** that were then rapidly diluted (to 0.0006% w/v) and drop casted on a mica substrate to investigate the size and topography of any self-assembled fibers formed under such conditions (SI-5.1). We have previously shown that AFM measurements on fibers formed from dilute drop-cast solutions yield comparable information to more experimentally challenging cryogenic transmission electron microscopy (cryo-TEM) and *in situ* small angle neutron scattering (SANS) methods.[27] No fibers were found for compounds **1** and **4**, which is in line with the observation that they did not self-assemble into gels. Compound **2** formed fibers with a diameter of 12.2±0.5 nm (in the dark) and when irradiated with 365 nm light the diameter of the fibers reduced to 7.2±0.4 nm, as measured by AFM (Figure 4b). Similarly, compound **3** formed thin sheet-like fibers with a diameter of 13.4±0.5 nm (in the dark) and 4.7±0.3 nm (after irradiation with 365 nm). On all occasions, the fibers appear longer than the maximum scan size used (5 x 5 μm). Scanning electron microscopy (SEM) was used to image the structures formed from **1**–**4** when more concentrated 1.2% (w/v) solutions (in the dark) were drop-cast onto silica (SI-5.2). The desiccated gels from **2** and **3** showed fiber-like surfaces, while the precipitates from compounds **1** and **4** were found to have crystal-like surfaces (SI-5.2.1, SI-5.2.4). If the solutions were

4

irradiated with 365 nm light prior to being drop-cast, the morphology observed for **2** and **3** changed from fibrous to crystalline, consistent with disassembly (see SI-5.2.2, SI-5.2.3).

The combination of TEM and cryo-TEM techniques were used to investigate the structural changes in the self-assembly of **2** and **3** before and after illumination with 365 nm light (SI-5.3). When comparing the cryo-TEM micrographs of the fibers from gels formed by **2** at 1.2% (w/v) in water before (Figure 4c) and after irradiation with 365 nm light (Figure 4d), a clear "thinning" of the fibers is observed, as the 29±7 nm wide sheets narrow down to 13±2 nm. These results are qualitatively consistent with the AFM analysis above, given that the latter are presumably dried out. This data is supported by conventional TEM analysis on 1.2% (w/v) solutions of **2** (SI-5.3.2). Compounds **1** and **4** did not show any fiber-like aggregates under these conditions. TEM analysis of **3** was less conclusive; conventional TEM did not show fibers but rather spherical, perhaps micellar-like objects prior to illumination that disintegrated upon illumination with 365 nm light (SI-5.3.3). The cryo-TEM micrographs of **3** before illumination showed very wide (≈ 400 nm) thin sheet like structures that do also become thinner (≈ 200 nm) after irradiation with 365 nm light (SI-5.3.6), which appear in some cases less than 1 μm long.

In an attempt to investigate the further the observed "thinning" and the mechanism of assembly/disassembly upon photoswitching, ^{1}H NMR studies were carried out on gels formed from **2** and **3** (SI 11.1). In both cases, switching the initially prepared gels to PSS_Z with a 365 nm light source resulted in sharp peaks indicating that **2** and **3** are freely mobile in the "sol" state, although in both cases, the signal intensity did not fully recover and some precipitates were visible in the NMR tube. For the "as prepared" gel from **2**, some residual broad signals from **2** were observed in the gel state which were not present in the PSS_E gel state that was generated upon switching the sol Z-**2** PSS_Z back to Z-**2** PSS_E with the 520 nm light source. This suggests that the gel initially formed by "as prepared" E-**2** differs significantly from the E-**2** PSS_E gel state, most likely as the they are formed by two different kinetic pathways. In contrast, no residual signals where observed in the "as prepared" gel from E-**3** but after switching to Z-**3** PSS_Z sol with a 365 nm light and then back to a E-**3** PSS_E state with a 520 nm light source resulted in a loss of the NMR signals and precipitation in the NMR tube. This indicates the poor solubility of **3** in water and that the initially observed gel formation for "as prepared" E-**3** is most likely a kinetic product, which up on rearrangement (apparent thinning) will start to precipitate in the PSS_Z state and even more so in the PSS_E state. For **2**, the aggregates in the sol Z-**2** PSS_Z state are probably different in nature and they then go on to form a gel again in the E-**2** PSS_E state but further studies will be required to elucidate this mechanism in details.

Photocontrolled dye release from gels

Hydrogels formed with compounds **2** or **3** can be used for controlled cargo release.[20] The fluorescent dye Rhodamine B was encapsulated during the hydrogel formation. The hydrogels were formed at the bottom of a quartz cuvette and allowed to gel overnight (see SI-3.15 for details). Water was carefully layered over the gels and the dye release was monitored by fluorescence emission spectroscopy (Figure 5). In the dark, gels of **2** and **3** released 15–25% of the dye load over 4 h (most of this due to the initial burst release of Rhodamine B). Upon

continuous irradiation with 365 nm light, the gels readily released the dye, reaching approximately 80–90% dye release over 4 h.
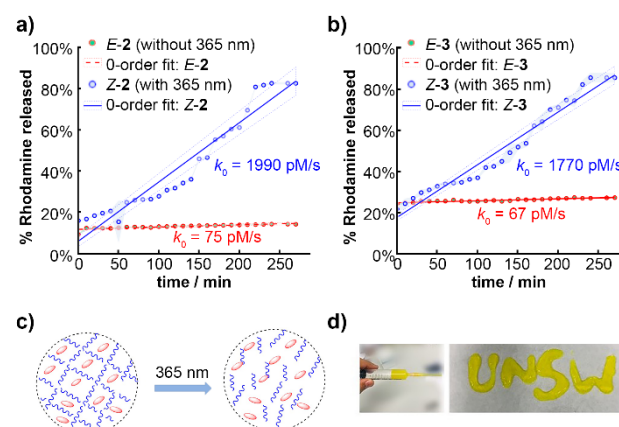

Figure 5. a) Release of Rhodamine B dye from hydrogels formed by a) **2** or b) **3** prepared by dissolving 1.2% (w/v) of **2** or **3** and 0.01% (w/v) of the dye in a solution of sodium hydroxide (98 mmol/L), followed by the addition of 0.16% (w/v) gδL. The samples were continually irradiated with UV light (365 nm) from above for the duration of the experiment. Release was monitored by fluorescence emission spectroscopy (λ_{ex} = 540 nm, λ_{em} = 576 nm), relative to complete release of the dye following by adding excess solvent to the top of the gel sample. Solid lines: Fitted release according to a zero-order kinetic model based on the zero-order rate constant (k_0) shown. Dotted lines indicate ±1 standard deviations (std) of the fitted zero-order kinetics. Circles: Averages of n = 3 repeat measurement of Rhodamine B releases. Shaded bands around the circles: ±1 std of the n = 3 repeat measurements. c) Cartoon representation of dye release from hydrogels upon irradiation with 365 nm light. d) Injectability: a gel formed by **3** can be pushed through a syringe to form a pattern.

The release of Rhodamine B from the hydrogel formed by **2** and **3** follow zero-order kinetics (k_0), which is usually considered desirable in second generation drug delivery systems.[28] More importantly, the rate of Rhodamine B release from gels formed by E-**2** and E-**3** increased more than 20-fold upon irradiation with a 365 nm light source, or from k_0 = 75±11 pM/s for E-**2** to 1990±110 pM/s for Z-**2** and k_0 = 67±8 pM/s for E-**3** to 1770±80 pM/s for Z-**3**. This can be readily explained by the fact that the 365 nm excitation triggers a gel → sol transition for these hydrogels over a period of ≈ 200 min (Figure 5). Hydrogels formed by **2** and **3** also show good thixotropic properties at 37 °C (SI-8.3), indicating that they can be readily injected with syringe (Figure 5d) – an advantageous property for application of these gels in light-controlled release systems.

Conclusion

Four photoswitchable arylazopyrazoles derivatives were synthesized, of which two form hydrogels at 1.2% w/v. The *meta*- and *para*-arylazopyrazoles **2** and **3**, respectively, are the lowest molecular weight photoswitchable hydrogelators reported to date. This is significant as small hydrogelators can reveal important details of gelation mechanisms by reducing degrees of freedom. Using a 365 nm light source, photoswitching of gels formed from the as synthesized E-**2** and E-**3**, to the corresponding photostationary state predominantly forms

5

(>90%) *Z*-**2** and *Z*-**3**. This results in nearly an order of magnitude reduction in the elastic (G') and loss (G'') modulus. Detailed microscopy studies, including cryo-TEM imaging, suggests that this transition is associated with significant thinning of the gel fibers and in the case of **3**, eventually irreversible precipitation or crystallization. Noting that the initially formed gel from *E*-**2** is different from those formed from photoisomerized *E*-**2** PSS$_E$, the rheological properties of **2** are reversible multiple times upon repeated switching between a 365 and 520 nm light sources, whereas for **3** they are not, and precipitation is observed. These observation highlight that gelation is a kinetic process and the starting points when gelation is triggered by a pH switch are significantly different from when the aggregates are photoisomerized. The light inducted gel→sol transition for gels formed from **2** and **3** can be used to accelerate more than 20-fold the release of an encapsulated dye in these gels, suggesting that these low-molecular hydrogelator could be used for light-controlled release systems in water at physiologically relevant pH. The insight that the structural simple and photoswitchable hydrogelators **2** and **3** have given here into the mechanism of hydrogel assembly and disassembly is likely to aid the design of other related light-controlled materials and systems in the future.

Acknowledgements

[1] K. Yonekura, S. Maki, D. G. Morgan, D. J. DeRosier, F. Vonderviszt, K. Imada, K Namba, *Science* **2000**, *290*, 2148-2152.

[2] E. J. Cohen, J. L. Ferreira, M. S. Ladinsky, M. Beeby, K. T. Hughes, *Science* **2017**, *356*, 197-200.

[3] D. Dattler, G. Fuks, J. Heiser, E. Moulin, A. Perrot, X. Yao, N. Giuseppone, *Chem. Rev.* **2019**, *120*, 310-433.

[4] a) X. Du, J. Zhou, J. Shi, B. Xu, *Chem. Rev.* **2015**, *115*, 13165-13307; (b) E. R. Draper, D. J. Adams, *Chem* **2017**, *3*, 390-410; c) S. Mondal, S. Das, A. K. Nandi, *Soft Matter* **2020**, *16*, 1404-1454.

[5] a) M. D. Segarra-Maset, V. J. Nebot, J. F. Miravet, B. Escuder, *Chem. Soc. Rev.* **2013**, *42*, 7086-7098; b) J. Hoque, N. Sangaj, S. Varghese, *Macromol. Biosci.* **2019**, *19*, 1800259.

[6] J. Hu, S. Liu, *Acc. Chem. Res.* **2014**, *47*, 2084-2095.

[7] M. Ikeda, T. Tanida, T. Yoshii, K. Kurotani, S. Onogi, K. Urayama, I. Hamachi, *Nat. Chem.* **2014**, *6*, 511-518.

[8] S. Wei, W. Lu, X. Le, C. Ma, H. Lin, B. Wu, J. Zhang, P. Theato, T. Chen, *Angew. Chem. Int. Ed.* **2019**, *58*, 16243-16251.

[9] X. Q. Dou, C. L. Feng, *Adv. Mat.* **2017**, *29*, 1604062.

[10] a) V. Balzani, A. Credi, M. Venturi, *Chem. Soc. Rev.* **2009**, *38*, 1542-1550; b) D. Habault, H. Zhang, Y. Zhao, *Chem. Soc. Rev.* **2013**, *42*, 7244-7256; c) E. R. Draper, D. J. Adams, *Chem. Commun.* **2016**, *52*, 8196-8206; d) X. Li, J. Fei, Y. Xu, D. Li, T. Yuan, G. Li, C. Wang, J. A. Li, *Angew. Chem. Int. Ed.* **2018**, *57*, 1903-1907; e) Z. L. Pianowski, *Chem.– Eur. J.* **2019**, *25*, 5128-5144.

[11] Z. Qiu, H. Yu, J. Li, Y. Wang, Y. Zhang, *Chem. Commun.* **2009**, 3342-3344.

[12] a) Y.-L. Zhao, J. F. Stoddart, *Langmuir* **2009**, *25*, 8442-8446; b) S. Tamesue, Y. Takashima, H. Yamaguchi, S. Shinkai, A. Harada, *Angew. Chem. Int. Ed.* **2010**, *49*, 7461-7464; c) G. Davidson-Rozenfeld, L. Stricker, J. Simke, M. Fadeev, M. Vázquez-González, B. J. Ravoo, I. Willner, *Polym. Chem.* **2019**, *10*, 4106-4115; d) A. Tabet, R. A. Forster, C. C. Parkins, G. Wu, O. A. Scherman, *Polym. Chem.* **2019**, *10*, 467-472.

[13] J. T. van Herpt, M. C. Stuart, W. R. Browne, B. L. Feringa, *Chem.‐Eur. J.* **2014**, *20*, 3077-3083.

[14] a) J. E. Stumpel, B. Ziółkowski, L. Florea, D. Diamond, D. J. Broer, A. P. Schenning, *ACS Appl. Mater. Inter.* **2014**, *6*, 7268-7274; b) C. Li, A. Iscen, L. C. Palmer, G. C. Schatz, S. I. Stupp, *J. Am. Chem. Soc.* **2020**, *142*, 8447-8453

[15] a) K. Peng, I. Tomatsu, A. Kros, *Chem. Commun.* **2010**, *46*, 4094-4096; b) A. A. Beharry, G. A. Woolley, *Chem. Soc. Rev.* **2011**, *40*, 4422-4437; c) Y. Huang, Z. Qiu, Y. Xu, J. Shi, H. Lin, Y. Zhang, *Org. Bio. Chem.* **2011**, *9*, 2149-2155; d) T. M. Doran, D. M.; Ryan, B. L. Nilsson, *Polym. Chem.* **2014**, *5*, 241-248; e) A. M. Rosales, K. M. Mabry, E. M. Nehls, K. S. Anseth, *Biomacromol.* **2015**, *16*, 798-806; f) Z. L. Pianowski, J. Karcher, K. Schneider, *Chem. Commun.* **2016**, *52*, 3143-3146; g) F. Xie, L. Qin, M. A. Liu, *Chem. Commun.* **2016**, *52*, 930-933; h) I.-N. Lee, O. Dobre, D. Richards, C. Ballestrem, J. M. Curran, J. A. Hunt, S. M. Richardson, J. Swift, L. S. Wong, *ACS. Appl. Mater. Inter.* **2018**, *10*, 7765-7776; i) A. M. Rosales, C. B. Rodell, M. H. Chen, M. G. Morrow, K. S. Anseth, J. A. Burdick, *Bioconjugate Chem.* **2018**, *29*, 905-913; j) M. E. Roth‐Konforti, M. Comune, M. Halperin‐Sternfeld, I. Grigoriants, D. Shabat, L. Adler‐Abramovich, *Macromol. Rapid. Commun.* **2018**, *39*, 1800588; k) C. Wang, K. Hashimoto, R. Tamate, H. Kokubo, M. Watanabe, *Angew. Chem. Int. Ed.* **2018**, *57*, 227-230; l) L. Li, J. M. Scheiger, P. A. Levkin, *Adv. Mater.* **2019**, *31*, 1807333; m) M. S. de Luna, V. Marturano, M. Manganelli, C. Santillo, V. Ambrogi, G. Filippone, P. Cerruti, *J. Colloid. Interf. Sci.* **2020**, *568*, 16-24; n) N. Higashi, R. Yoshikawa, T. Koga, *RSC Adv.* **2020**, *10*, 15947-15954.

[16] F. Tong, S. Chen, Z. Li, M. Liu, R. O. Al-Kaysi, U. Mohideen, Y. Yin, C. J. Bardeen, *Angew. Chem. Int. Ed.* **2019**, *58*, 15429-15434.

[17] a) J. V. Accardo, J. A. Kalow, *Chem. Sci.* **2018**, *9*, 5987-5993; b) J. Karcher, Z. L. Pianowski, *Chem.‐ Eur. J.* **2018**, *24*, 11605-11610; c) F. Zhao, A. Bonasera, U. Nöchel, M. Behl, D. Bléger, *Macromol. Rapid. Commun.* **2018**, *39*, 1700527; d) X. Tong, Y. Qiu, X. Zhao, B. Xiong, R. Liao, H. Peng, Y. Liao, X. Xie, *Soft Matter* **2019**, *15*, 6411-6417.

[18] C. W. Chu, L. Stricker, T. M. Kirse, M. Hayduk, B. J. Ravoo, *Chem.‐ Eur. J.* **2019**, *25*, 6131-6140.

[19] a) C. E. Weston, R. D. Richardson, P. R. Haycock, A. J. P. White, M. J. Fuchter, *J. Am. Chem. Soc.* **2014**, *136*, 11878-11881; b) J. Calbo, C. E. Weston, A. J. P. White, H. S. Rzepa, J. Contreras-García, M. J. Fuchter, *J. Am. Chem. Soc.* **2017**, *139*, 1261-1274; c) S. Crespi, N. A. Simeth, B. König, *Nat. Rev. Chem.* **2019**, *3*, 133-146; d) R. S. Gibson, J. Calbo, M. J. Fuchter, *Chem. Photo. Chem.* **2019**, *3*, 372-377; e) M. A. Gerkman, R. S. Gibson, J. Calbo, Y. Shi, M. J. Fuchter, G. G. Han, *J. Am. Chem. Soc.* **2020**, *142*, 8688-8695.

[20] C.-W. Chu, B. J. Ravoo, *Chem. Commun.* **2017**, *53*, 12450-12453.

[21] a) D. K. Kumar, D. A. Jose, P. Dastidar, A. Das, *Langmuir*, **2004**, *20*, 10413-10418. b) J. Shi, Y. Gao, Z. Yang, B. Xu, *Beilstein J. Org. Chem.* **2011**, *7*, 167-172; b) A. J. Kleinsmann, B. J. Nachtsheim, *Chem. Commun.* **2013**, *49*, 7818-7820.

[22] M. A. Spackman, D. Jayatilaka, *CrystEngComm* **2009**, *11*, 19-32.

[23] A. D. Martin, J. Britton, T. L. Easun, A. J. Blake, W. Lewis, M. Schröder, *Cryst. Grow. Des.* **2015**, *15*, 1697-1706.

[24] D. J. Adams, M. F. Butler, W. J. Frith, M. Kirkland, L. Mullen, P. Sanderson, *Soft Matter* **2009**, *5*, 1856-1862.

[25] S. R. Raghavan, B. H. Cipriano in *Molecular gels* (Eds.: R. G. Weiss, P. Terech), Springer, Dordrecht, **2006**; pp. 241-252.

[25] A. D. Martin, J. P. Wojciechowski, A. B. Robinson, C. Heu, C. J. Garvey, J. Ratcliffe, L. J. Waddington, J. Gardiner, P. Thordarson, *Sci. Rep.* **2017**, *7*, 43947.

[26] K. Park, *J. Controlled Release* **2014**, *190*, 3-8.

Entry for the Table of Contents

Insert graphic for Table of Contents here.
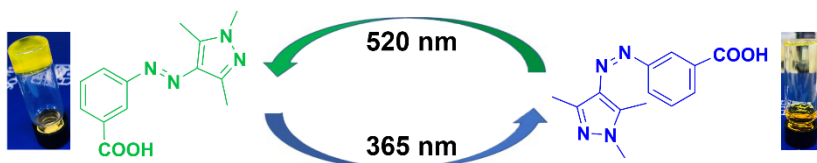
Tiny switchable gelators: Small photoswitchable (MW 258 g/mol) arylazopyrazoles form self-assembled gels in water that can be reversibly cycled between a gel and solution state using two different excitation wavelengths that causing "thinning" of the gel fibers upon the light induced *E* to *Z* isomerisation.

Institute and/or researcher Twitter usernames: @FayazAliLarik1 @LucyFillbrook @SandraNurttila @doc_martinaus @JonBeves @PalliThordarson